Synchronous diffuse large B-cell lymphoma and mantle cell lymphoma

de Groot, Fleur A; de Haan, Lorraine M; de Groen, Ruben A L; Heijmen, Linda; van Wezel, Tom; van Eijk, Ronald; Bohmer, Lara; Bot, Freek; Ten Berge, Rosita L; Diepstra, Arjan

Published in:
Leukemia & lymphoma

DOI:
10.1080/10428194.2021.2015589

Publication date:
2022

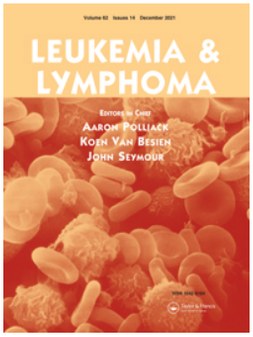

Leukemia & Lymphoma

ISSN: (Print) (Online) Journal homepage: https://www.tandfonline.com/loi/ilal20

Synchronous diffuse large B-cell lymphoma and mantle cell lymphoma: support for low-threshold biopsies and genetic testing

Fleur A. de Groot, Lorraine M. de Haan, Ruben A. L. de Groen, Linda Heijmen, Tom van Wezel, Ronald van Eijk, Lara Bohmer, Freek Bot, Rosita L. ten Berge, Arjan Diepstra, Hendrik Veelken, Arjen H. G. Cleven, Patty M. Jansen & Joost S. P. Vermaat

To cite this article: Fleur A. de Groot, Lorraine M. de Haan, Ruben A. L. de Groen, Linda Heijmen, Tom van Wezel, Ronald van Eijk, Lara Bohmer, Freek Bot, Rosita L. ten Berge, Arjan Diepstra, Hendrik Veelken, Arjen H. G. Cleven, Patty M. Jansen & Joost S. P. Vermaat (2021): Synchronous diffuse large B-cell lymphoma and mantle cell lymphoma: support for low-threshold biopsies and genetic testing, Leukemia & Lymphoma, DOI: 10.1080/10428194.2021.2015589

To link to this article: https://doi.org/10.1080/10428194.2021.2015589

Published online: 21 Dec 2021.

LEUKEMIA & LYMPHOMA
https://doi.org/10.1080/10428194.2021.2015589

Taylor & Francis
Taylor & Francis Group

LETTER TO THE EDITOR

Synchronous diffuse large B-cell lymphoma and mantle cell lymphoma: support for low-threshold biopsies and genetic testing

Fleur A. de Groot[a]* , Lorraine M. de Haan[b]*, Ruben A. L. de Groen[a], Linda Heijmen[c], Tom van Wezel[b], Ronald van Eijk[b], Lara Bohmer[d], Freek Bot[e], Rosita L. ten Berge[e], Arjan Diepstra[f], Hendrik Veelken[a], Arjen H. G. Cleven[b], Patty M. Jansen[b] and Joost S. P. Vermaat[a]

[a]Department of Hematology, Leiden University Medical Center, Leiden, The Netherlands; [b]Department of Pathology, Leiden University Medical Center, Leiden, The Netherlands; [c]Department of Radiology, Leiden University Medical Center, Leiden, The Netherlands; [d]Department of Hematology, Haga Hospital, The Hague, The Netherlands; [e]Department of Pathology, Haga Hospital, The Hague, The Netherlands; [f]Department of Pathology, University of Groningen, University Medical Center Groningen, Groningen, The Netherlands

ARTICLE HISTORY Received 24 September 2021; revised 22 November 2021; accepted 29 November 2021

Transformation of an indolent B-cell lymphoma into a clonally related aggressive large B-cell lymphoma is relatively common [1]. Composite lymphomas, the simultaneous appearance of two (or more) clonally unrelated lymphomas occurring in the same tissue site or organ, are also described before [2–4]. However, to our knowledge, a synchronous presence of two clinically and genetically different aggressive B-cell lymphoma subtypes (i.e. diffuse large B-cell lymphoma (DLBCL) and mantle cell lymphoma (MCL)) in two distinct anatomical locations is currently unknown. Both lymphomas have specific morphological, immunohistochemical (IHC), and genetic characteristics. Although, CD5 negative MCL and cyclin D1 positive DLBCL are described, complicating clear differentiation between both entities and additional genetic evaluation is required [5]. This report is the first to describe the exclusive presence of a synchronous DLBCL and MCL, with corresponding distinct clinical and radiological features. Extensive genomic analyses demonstrated that DLBCL and MCL were genetically unrelated. Consequently and in contrast to composite lymphomas, appropriate treatment strategies and response evaluation need to be tailored to both synchronous lymphoma entities.

A 56-year-old man presented with abdominal complaints for months and general malaise, extensive night sweats and palpable lymph nodes since weeks. A PET-CT scan was performed and analyzed using the EARL FDG-PET/CT acquisition launched by the European Organization for Research and Treatment of Cancer (EORTC) imaging group to assist imaging sites in meeting the standard requirements specified in the guideline. The intensity PET-CT projection showed multiple lesions with varying maximum standardized uptake values (SUVmax), indicating that these lesions reflect different disease entities (Figure 1(A,B)). Intense FDG-avid lymphadenopathy was seen inguinal, cervical and axillar (SUVmax 16.6, 19.1, and 25.1, respectively), suggesting an aggressive disease (mean SUVmax 20.3) [6]. The spleen, hepatic, and parailiac lymph nodes, and the sigmoid colon showed moderate FDG-avidity (SUVmax of 3.6, 5.0, 3.7, and 4.3, respectively). These light gray lesions (mean SUVmax 4.2) were expected to be of more indolent character. The differential intensity of FDG-avid lesions, along with acute and chronic symptoms and iron deficiency anemia caused by intestine involvement, was suspect for distinct disease entities, and consequently the axilla and colon lesions were biopsied. These two lesions were biopsied and it has been assumed that these represent all other lesions with comparable FDG-avidity because taking more biopsies is not patient friendly, clinically inefficient and the chances of having a third synchronous lymphoma are negligibly small.

Histologic examination of the axillary lymph node showed an architectural effacement by a diffuse proliferation of atypical large lymphoid cells (Figure 1(C)). The lesional cells contained scant cytoplasm with large irregular nuclei and prominent nucleoli, frequently with mitotic figures and apoptosis. The colon samples demonstrated submucosal diffuse monomorphic proliferations of small to medium sized lymphoid cells with slightly irregular and indented nuclei (Figure 1(C)) with inconspicuous nucleoli. Mitosis and apoptosis were infrequent. Next, as we have described before, IHC and (Fluorescent) In Situ Hybridization ((F)ISH) analyses were performed following the latest WHO Classification for Hematological

CONTACT Joost S. P. Vermaat j.s.p.vermaat@lumc.nl Department of Hematology, Leiden University Medical Center, PO Box 9600, 2300 RC Leiden, The Netherlands
*Both authors contributed equally to this work.
Supplemental data for this article can be accessed here.

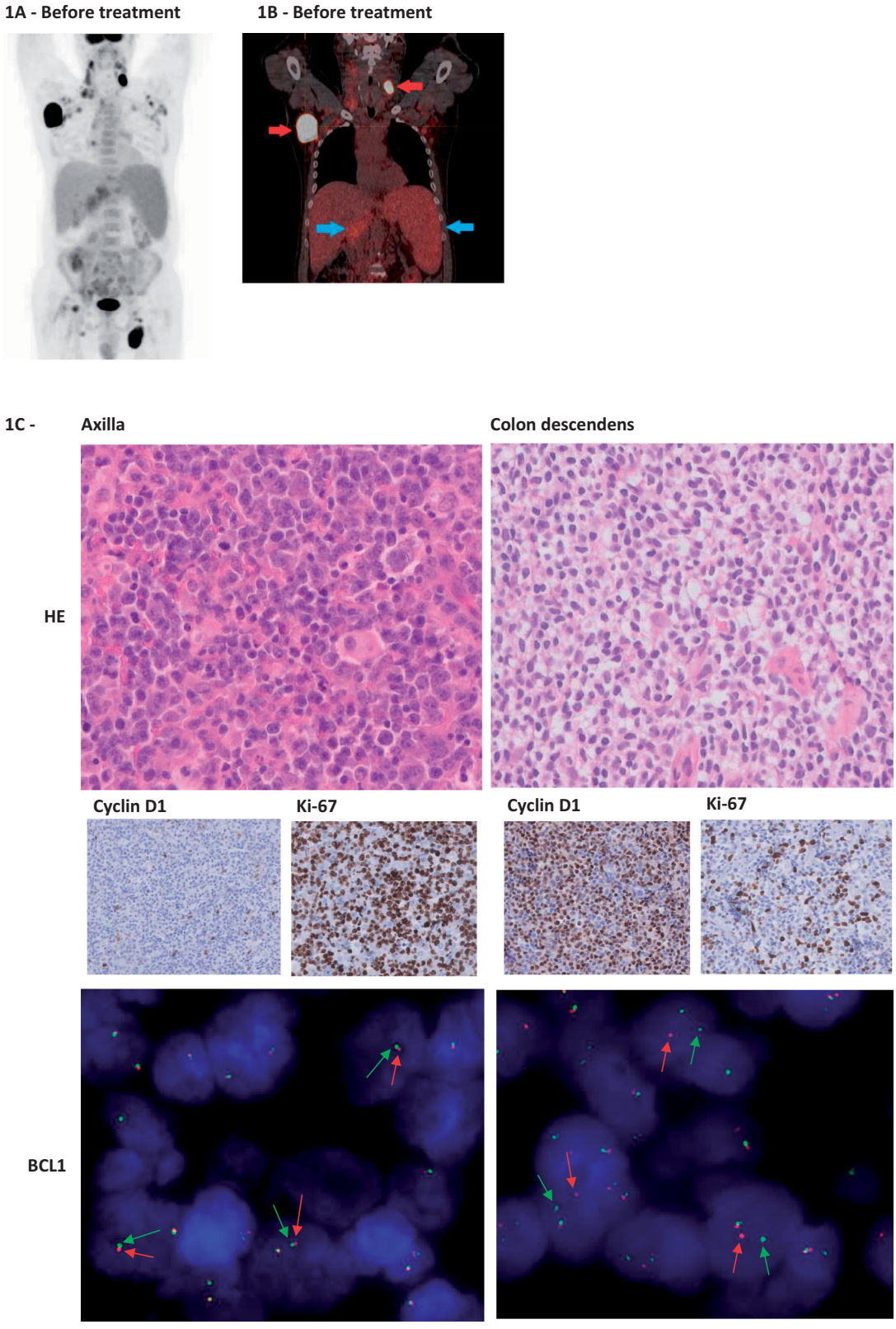

Figure 1. (A) Maximal intensity PET-CT EARL acquisition depicting SUVmax of different lesions before treatment. Intense FDG-avid lymphadenopathy (black lesions) was seen inguinal, cervical, and axillar. Moderate FDG-avidity (gray lesions) was seen in the spleen, hepatic and para-iliac lymph nodes and the sigmoid colon. (B) Highlighted DLBCL suspected lesions with arrows cervical and axillar and MCL suspected lesions with arrows in the liver and the spleen. (C) Immunohistochemistry on DLBCL and MCL sample with hematoxylin and eosin, cyclin D1, and Ki-67 showing distinct staining expressions. FISH analysis demonstrated a BCL1 rearrangement in MCL (indicated by separated arrows) but not in DLBCL (indicated by linked arrows).

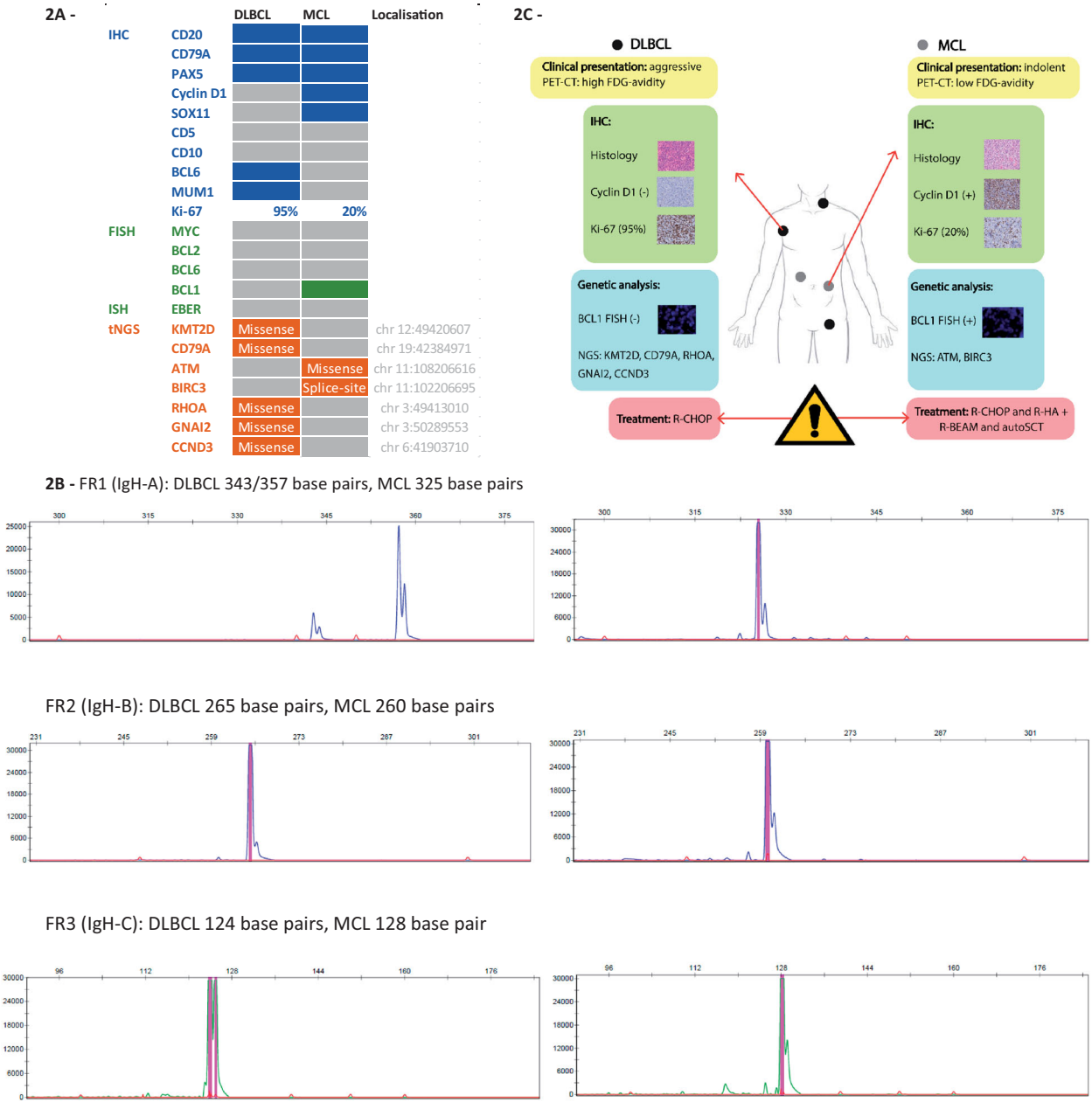

Figure 2. (A) Summarized results of immunohistochemistry, (F)ISH analysis, and targeted next generation sequencing. Dark squares depict a positive IHC, (F)ISH, or identified variant result, light squares represents a negative IHC, (F)ISH, or wildtype gene. (B) Clonality assessment in FR1 (IgH-A), FR2 (IgH-B), and FR3 (IgH-C) demonstrated IgH profiles of the two clonally unrelated samples. (C) Schematic overview emphasizing the necessity for low-threshold biopsies in appropriate diagnostic procedures of suspect clinical course and lesions with differential FDG-avidity, thereby guiding therapeutic strategies.

Malignancies [7]. Thin slides of 3 μm of patients' FFPE tissues were stained for antibody expression (Dako Omnis, Glostrup, Denmark), using the Dako Autostainer Link 48 (Dako, Glostrup, Denmark), according to standard procedures. Both samples showed strong diffuse positivity for the B-cell markers CD20, CD79A, and PAX5. The axilla showed no cyclin D1 and SOX11 expression in the lesional cells, while the colon showed both strong cyclin D1 and SOX11 staining. Both lesions were negative for CD5. Opposed to very high Ki-67 proliferation (∼95%) of the axilla, the colon showed low Ki-67 proliferation (∼20%). Given IHC negativity for CD10 and positivity for BCL6 and MUM1, the axillary sample was classified as DLBCL with a non-germinal center B-cell phenotype (Hans algorithm) [8]. The colon tissue demonstrated negativity for CD10, BCL6, and MUM1. Rearrangement of *MYC*, *BCL2*, *BCL6*, and *CCND1* were assessed with Vysis Dual Color Break Apart Rearrangement Probes from Abbott using the Dako Histology FISH Accessory Kit [9]. Both samples showed no *MYC*, *BCL2*, or *BCL6* rearrangement and EBER was negative. A *BCL1* rearrangement was identified in the colon but not in the axilla (Figure 1(C)),

underlining the diagnosis MCL, without a blastoid phenotype. Combining these pathological characteristics with literature on FDG-avidity reporting that the mean SUVmax in DLBCL is 21.8 with a standard deviation of 9.1 and the median SUVmax of MCL is 7.4 (ranging from 1.8 to 33.8) confirmed that both pathology and the PET-CT results fit the diagnosis of DLBCL in the intense axillary lesion and MCL in the moderate lesion in the colon [10]. As done before, cell-of-origin (COO) classification was performed by gene-expression-profiling using a custom-made Lymph2Cx NanoString panel covering 20 genes for COO classification. Gene expression data were normalized by using five Lymph2Cx housekeeping genes. This COO categorization demonstrated an intermediate subtype for DLBCL (Supplementary methods) [11]. Clonal rearrangement analysis of IgH-/IgK-locus (Supplementary methods) showed no clonal relation between DLBCL and MCL (Figure 2(B)).

Mutational profiles were analyzed using an in-house targeted next-generation sequencing (tNGS) panel (BLYMF200), including 200 lymphoma-relevant genes (Supplementary methods and Table S1), as extensively described before [12]. Average read count was 1591 (range, 0–11995; Supplementary Table S2). Variants with coverage $\geq$100 reads and allele frequency of $\geq$5% were functionally annotated. For DLBCL, *KMT2D*, *CD79A*, *RHOA*, *GNAI2*, and *CCND3* mutations were identified corresponding with a non-GCB phenotype (Figure 2(A,C)) [13]. *ATM* and *BIRC3* mutations underscored the MCL diagnosis, *TP53* was wildtype [14]. Since no aberrations were noted in peripheral blood mononuclear cells (PBMCs), identified mutations were all considered somatic variations. Overall, the identification of different molecular profiles along with confirmation that both samples were clonally different, in addition to discriminative morphological and IHC features, illustrates the presence of a synchronous genetically unrelated double B-cell lymphoma (i.e. DLBCL and MCL). Considering both synchronous lymphoma entities, treatment was adapted to alternate immuno-chemotherapy R-CHOP (i.e. rituximab, cyclophosphamide, doxorubicin, vincristine, and prednisone) for DLBCL with high-dose cytarabine for MCL (Figure 2(C)). It was intended to consolidate through intensive myeloablative chemotherapy and autologous stem cell rescue. Due to severe bowel toxicity caused by induction chemotherapy, this intensive consolidation part was rejected. Subsequent evaluation with PET-CT scan showed a persistent intense FDG-avid axillary lesion and moderate FDG-avidity of the colon. Again, tissue biopsies were obtained from both lesions, demonstrating a reactive inflammatory environment in the axilla and persistent MCL in the colon. Given the initial presence of bulky disease in the axilla and a persistent intense FDG-avid lesion, local radiotherapy was given additionally (35 Gy). As MCL persisted in the colon, lenalidomide and rituximab (LR) was started as maintenance therapy. This was rationally based on the genetic profiles and substantial response rates of LR in both DLBCL and MCL [15]. After three cycles, colonoscopy demonstrated a significant clinical response of the colon. This demonstrates that response evaluation for both disease entities should be assessed individually and as part of the synchronous lymphoma. In contrast to composite lymphomas, for synchronous lymphomas individual histological assessment of lesions with different PET-avidity is important to optimize targeted treatment and response evaluation per lymphoma subtype and localization. The presented unique case demonstrated this individualized approach for both lymphoma subtypes and anatomical sites by adjuvant radiotherapy of the axillary PET avid lesions and the initiation of LR for the persistent MCL bowel lesions.

This study is the first to present a synchronous genetically unrelated double B-cell lymphoma. Since DLBCL and MCL are treated differently, significant diagnostic procedures including extensive genetic analyses are of vital importance. As also with composite lymphomas, clinical presentations are generally more straightforward with similar FDG-avid intensities at individual PET-CT scans. In case of different clinical courses and/or FDG-avid intensities at PET-CT scan, the most intense lesion is usually biopsied. In contrast, this study illustrates the need to carefully evaluate both clinical course and different FDG-avid intensities in multidisciplinary consultations and stresses the necessity of low-threshold biopsies and comprehensive genetic testing to adapt the optimal therapeutic strategy and response evaluations. Hence, clinical and radiological presentations were suspicious for different disease entities, biopsies of both lesions with distinct FDG-avid intensity were fundamental in the diagnostic procedure. Integral and comprehensive analyses of morphology, IHC and FISH, supplemented by tGEP, clonality analysis and tNGS using the BLYMF200 panel demonstrated genetically distinct B-cell lymphoma subtypes. Different mutational profiles in different pathways were identified, as DLBCL harbored mutated *KMT2D*, *CD79A*, *RHOA*, *GNAI2*, and *CCND3*, while MCL contained *BCL1* rearrangement and *ATM* and *BIRC3* aberrations. Consequently, the therapeutic strategy was adapted to both DLBCL and MCL. Without being an issue for composite lymphomas, response evaluations were performed individually for both entities and as part of the synchronous lymphoma entities to optimize further treatment strategies. Conclusively, in contrast to composite lymphomas, this study advocates for the need of low-threshold tissue examination including extensive genetic analysis if a clinical and radiological suspicion of two disease entities is present, thereby guiding optimal therapeutic strategies with subsequent response evaluations targeting both synchronous lymphoma entities.

Authors contributions

L.B., H.V., and J.S.P.V. diagnosed, treated, and included the patient. L.H. assessed the radiology. F.B., R.L.B., P.M.J.,

A.H.G.C., and L.M.H. assessed the pathology. A.D. executed the tGEP/Nanostring. R.A.L., T.W., R.E., and J.S.P.V. designed and optimized the tNGS sequencing panel. F.A.G., R.A.L., and R.E. analyzed and interpreted the molecular data. L.M.H., F.A.G., and J.S.P.V. analyzed and interpreted the data and wrote the manuscript.

Acknowledgements

The authors thank Dina Ruano, Karin Kleiverda, and Demi van Egmond of the Department of Pathology of the LUMC for their technical assistance.

Disclosure statement

None of the authors declare any conflict of interest.

Funding

The author(s) reported there is no funding associated with the work featured in this article.

ORCID

Fleur A. de Groot http://orcid.org/0000-0001-9940-2891
Joost S. P. Vermaat http://orcid.org/0000-0002-1628-6256

References

[1] Montoto S, Fitzgibbon J. Transformation of indolent B-cell lymphomas. J Clin Oncol. 2011;29(14):1827–1834.
[2] Miyaoka M, Kikuchi T, Carreras J, et al. Composite follicular lymphoma and CD5-positive nodal marginal zone lymphoma. J Clin Exp Hematop. 2016;56(1):55–58.
[3] Mohammad F, Garcia G, Kedia S, et al. Composite diffuse large B-cell and mantle cell lymphoma: a case report. Cureus. 2017;9(1):e963.
[4] Ho AK, Teman CJ, Smith GP, et al. Composite mantle cell and diffuse large B-cell lymphoma: report of two cases. Int J Surg Pathol. 2011;19(5):643–648.
[5] Liu Z, Dong HY, Gorczyca W, et al. CD5- mantle cell lymphoma. Am J Clin Pathol. 2002;118(2):216–224.
[6] Adams HJ, de Klerk JM, Fijnheer R, et al. Prognostic superiority of the National Comprehensive Cancer Network International Prognostic Index over pretreatment whole-body volumetric-metabolic FDG-PET/CT metrics in diffuse large B-cell lymphoma. Eur J Haematol. 2015;94(6):532–539.
[7] Swerdlow SH, Campo E, Pileri SA, et al. The 2016 revision of the world Health Organization classification of lymphoid neoplasms. Blood. 2016;127(20):2375–2390.
[8] Hans CP, Weisenburger DD, Greiner TC, et al. Confirmation of the molecular classification of diffuse large B-cell lymphoma by immunohistochemistry using a tissue microarray. Blood. 2004;103(1):275–282.
[9] Vermaat JS, Somers SF, de Wreede LC, et al. MYD88 mutations identify a molecular subgroup of diffuse large B-cell lymphoma with an unfavorable prognosis. Haematologica. 2020;105(2):424–434.
[10] Bailly C, Carlier T, Berriolo-Riedinger A, et al. Prognostic value of FDG-PET in patients with mantle cell lymphoma: results from the LyMa-PET project. Haematologica. 2020;105(1):e33–e36.
[11] Scott DW, Wright GW, Williams PM, et al. Determining cell-of-origin subtypes of diffuse large B-cell lymphoma using gene expression in formalin-fixed paraffin-embedded tissue. Blood. 2014;123(8):1214–1217.
[12] de Groen RA, van Eijk R, Boehringer S, et al. Frequent mutated B2M, EZH2, IRF8, and TNFRSF14 in primary bone diffuse large B-cell lymphoma reflect a GCB phenotype. Blood Adv. 2021;5(19):3760–3775.
[13] Chapuy B, Stewart C, Dunford AJ, et al. Molecular subtypes of diffuse large B cell lymphoma are associated with distinct pathogenic mechanisms and outcomes. Nat Med. 2018;24(5):679–690.
[14] Bea S, Valdes-Mas R, Navarro A, et al. Landscape of somatic mutations and clonal evolution in mantle cell lymphoma. Proc Natl Acad Sci U S A. 2013;110(45):18250–18255.
[15] Wang M, Fowler N, Wagner-Bartak N, et al. Oral lenalidomide with rituximab in relapsed or refractory diffuse large cell, follicular and transformed lymphoma: a phase II clinical trial. Leukemia. 2013;27(9):1902–1909.